Proceedings World Geothermal Congress 2020+1
Reykjavik, Iceland, April - October 2021

Heat and Solute as Tracers for Designing Sustainable Groundwater Heat Pump Systems

Ji-Young Baek[1)], Byeong-Hak Park[2)], Hae-Rim Oh[1)], Dugin Kaown[1)], Seong-Sun Lee[1)], Kang-Kun Lee[1)]

[1)] School of Earth and Environmental Science, Seoul National University, Republic of Korea

[2)] Radioactive Waste Disposal Research Division, Korea Atomic Energy Research Institute, Republic of Korea

kklee@snu.ac.kr

Keywords: Groundwater, Groundwater Heat Pump, Solute, Heat, Tracer Test

ABSTRACT

Higher efficiency and smaller space requirements make groundwater heat pump (GWHP) systems much preferable, especially for large heating and cooling plants. The design of GWHP systems is, however, highly dependent on the aquifer properties mainly due to the direct use of groundwater. Therefore, the aquifer characterization has a great importance in assessing the temperature anomalies and designing the efficient and sustainable GWHP systems. In this study, a total of 52 transport experiments on sub-meter scale using both heat and solute as tracers were performed at various background flow velocities ($Re < 0.37$) to characterize the physical properties of fully saturated porous media ($d_{50} = 0.76$ and $C_u = 1.50$). Since heat and solute have different transport regimes at the same Darcy fluxes, this can enhance the characterization of the flow and transport processes and the prediction of the thermal plume propagation. Fluid EC and temperature time series data were analyzed by five mathematical models to derive the velocities and the dispersion coefficients of tracers. The estimated properties from solute transport experiments were compared with those from heat transport experiments. The results of this work can deepen our understanding of flow and transport processes in porous media and improve the aquifer characterization and the design of the GWHP systems.

1. INTRODUCTION

The groundwater heat pump (GWHP) system is an open-loop ground source heat pump system that uses relatively stable temperature of groundwater as an energy source or sink. GWHP has been regarded preferable for heating and cooling systems of large buildings because of its smaller space requirement and higher efficiency. Because of a direct use of groundwater in GWHP systems, thermal impacts of the system are highly related to the aquifer properties such as hydraulic conductivity, groundwater flow velocity, porosity and thermal dispersion. For example, it has been shown that the groundwater flow velocity affects the thermal plume size in terms of both length and width (Piga et al., 2017). Also previous researches have concluded the importance of thermal dispersion in designing sustainable GWHP (Park et al., 2015). Therefore, aquifer characterization has a great importance in assessing the thermal impacts and designing the sustainable GWHP systems.

Tracer experiments have provided insights for determining aquifer characteristics and understanding the transport processes (Ma et al., 2012; Sarris et al., 2018). Especially, comparison between solute and heat tracer tests has several advantages. Vandenbohede et al. (2009) conducted field push-pull tests using both heat and chloride ion as tracers and pointed out that more accurate parameter estimation can be available by using both heat and solute tracers. Ma et al. (2012) described the cost efficiency by using both tracers to study heterogeneous aquifer especially in a vertical direction. Rau et al. (2012) performed laboratory tracer tests using both tracers to deepen understanding of dispersive transport in the subsurface. Bandai et al. (2017) also carried out laboratory solute and heat tracer tests and explained that particle size affects thermal dispersion only.

In this study, a total of 52 transport experiments on sub-meter scale using both heat and solute as tracers were performed at various background flow velocities ($Re < 0.37$) to characterize the physical properties of a fully saturated porous medium ($d_{50} = 0.76$ and $U = 1.50$). Since heat and solute have different transport regimes at the same Darcy fluxes, this can enhance the characterization of the flow and transport processes and the prediction of the thermal plume propagation. Fluid EC and temperature time series data were analyzed by mathematical models to derive the velocities and the dispersion coefficients of tracers. The estimated properties from solute transport experiments were compared with those from heat transport experiments.

2. METHODOLOGY

2.1 Laboratory Tracer Experiments

The laboratory experimental device was constructed for the investigation of solute and heat transport in a porous medium. The sand was packed in an acrylic glass tank as a porous medium and two constant head chambers were installed to generate the horizontal flow. In the monitoring system of the experimental device, RTD sensors and microelectrodes were installed at fixed locations (Fig. 1). The temperature data and fluid EC data were logged in a real time through the LabVIEW and PodVu programs. More details about the experimental device are described in Park et al. (2018).

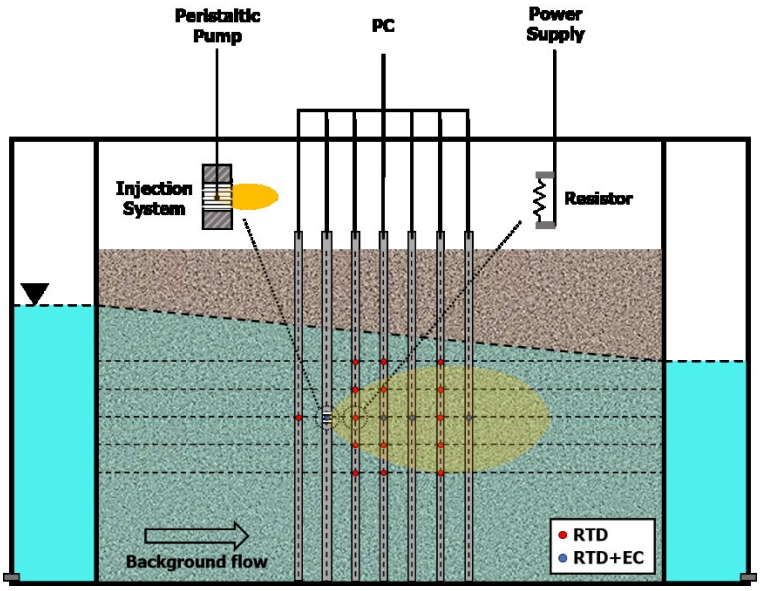

Figure 1: Schematic diagram of laboratory experimental device.

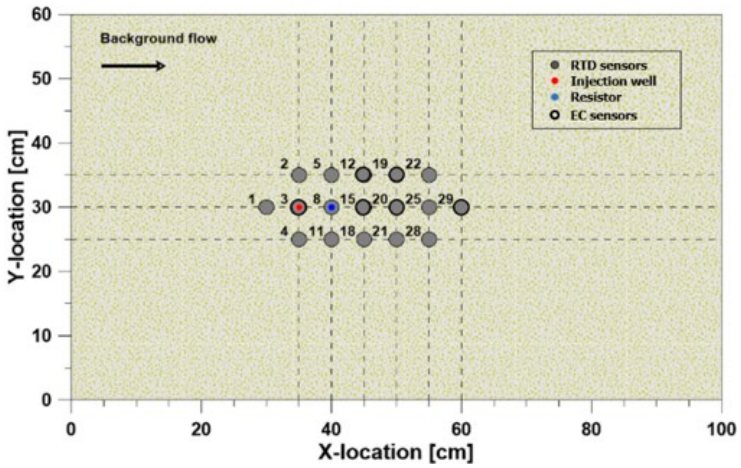

Figure 2: Top view of sensor and source location. (modified from Park et al., 2018)

The properties of the porous medium, such as mean grain size, porosity and hydraulic conductivity, are very important in understanding transport processes through the tracer tests. Because of the importance, sieve analysis was conducted, before the hydraulic tests, to evaluate mean grain size and the coefficient of uniformity of the medium. Also, porosity was determined from the mean value of fifty repeat experiments with samples of the sand. After those experiments, a hydraulic conductivity of the medium was calculated by linear regression analysis on constant head permeability tests results (Table 1).

Table 1. Physical properties of used sand in this study.

Parameter	Unit	Value	Source
Mean grain size	mm	0.76	Grain size analysis
Coefficient of uniformity	-	1.50	Grain size analysis
Effective porosity	-	0.374	Experiments
Density of sand	kg m^{-3}	2500	Experiments
Hydraulic conductivity	m s^{-1}	0.003228	Permeability tests

Laboratory tracer tests were carried out under various Darcy velocities ranging from $9.412 \cdot 10^{-5}$ to $4.254 \cdot 10^{-4}$ [m s^{-1}] for both solute and heat tracers. Sodium chloride (NaCl, 99.5%, Junsei Chemical, Japan) solution was instantaneously injected into the sand tank with a rate of 50 [ml min^{-1}] through a peristaltic pump (Minipuls 3, Gilson, USA) as a solute tracer. Concentration of the solution was determined to be 500 ppm to avoid a density effect (Schincariol and Schwartz, 1990). A resistor supplied with the source of 4.517 W continuously generated the heat at a fixed location during the heat tracer tests. Especially, in case of heat tracer, the tracer experiments under no-flow condition were needed to be pre-performed for obtaining thermal diffusivity of the medium because thermal property of the medium cannot be specified unlike the diffusion coefficient of sodium chloride.

Front velocities of tracers are calculated with specific discharge which measured from outlet tank by Eq. 1 and 2 for solute and heat tracer, respectively (see Rau et al., 2012). Also experimental conditions of laboratory tracer tests were evaluated by dimensionless numbers such as Reynolds number and Peclet number. Reynolds number is the ratio of inertial forces to viscous forces within a fluid and is defined in a porous medium as Eq. 3 (de Marsily, 1986). Peclet number is a quantitative comparison between the advective and diffusive transports. Solute Peclet number in a porous medium is given as Eq. 4 (de Marsily, 1986) and thermal Peclet number in a porous medium is expressed by Eq. 5 (de Marsily, 1986; Park et al., 2018).

$$v^s = \frac{\mathrm{q}}{n_e} \tag{1}$$

$$v^t = \frac{\rho_w c_w}{\rho_b c_b} q \tag{2}$$

$$Re = \frac{\rho_w q d_{50}}{\mu_w} \tag{3}$$

$$Pe^s = \frac{v^s d_{50}}{D_f} \tag{4}$$

$$Pe^t = \frac{\rho_w c_w q d_{50}}{\lambda} \tag{5}$$

2.2 Transport Parameters Estimation

The observed breakthrough curves (BTCs) of fluid EC and temperature were analyzed by solute and heat forward models. Analytical modeling was carried out based on non-linear least square method for the estimates of the transport parameters by fitting the analytical solutions of transport equations to the breakthrough curves. Transport of solute and heat can be explained in a similar form under local thermal equilibrium condition (Eqs. 6 and 7, also see de Marsily, 1986; Rau et al., 2012). And analytical solutions to Eqs. 6 and 7 (under specific boundary conditions) are described in Eqs. 8 and 9 (Hunt, 1978; Rau et al., 2012).

$$D^s \nabla^2 C - v^s \nabla \cdot C = \frac{\partial \mathrm{C}}{\partial t} \tag{6}$$

$$D^t \nabla^2 T - v^t \nabla \cdot T = \frac{\partial \mathrm{T}}{\partial t} \tag{7}$$

$$\mathrm{C(x,y,z,t)} = \frac{M}{8\pi n_e R D_y^s} \cdot \exp\left(\frac{x v^s}{2D_x^s}\right)\left\{\exp\left(-\frac{R v^s}{2D_x^s}\right) erfc\left(\frac{R - v^s t}{2\sqrt{D_x^s t}}\right) + \exp\left(\frac{R v^s}{2D_x^s}\right) erfc\left(\frac{R + v^s t}{2\sqrt{D_x^s t}}\right)\right\} \tag{8}$$

$$\mathrm{T(x,y,z,t)} = \frac{Q}{8\pi R D_y^t \rho c} \cdot \exp\left(\frac{x v^t}{2D_x^t}\right)\left\{\exp\left(-\frac{R v^t}{2D_x^t}\right) erfc\left(\frac{R - v^t t}{2\sqrt{D_x^t t}}\right) + \exp\left(\frac{R v^t}{2D_x^t}\right) erfc\left(\frac{R + v^t t}{2\sqrt{D_x^t t}}\right)\right\} \tag{9}$$

In case of fluid EC data, they were integrated to adopt Eq. 8 for better comparison with heat tracer tests. Also, they were normalized since there were difficulties in converting the EC to the concentration. Generally, EC values and concentration have a linear relationship, but it is hard to obtain a constant coefficient in situ because of its sensitivity to hydraulic pressure. Therefore Eq. 8 was modified for applying the solute forward model to the preprocessed solute BTCs (Eq. 10, also see Rau et al., 2012). All the fitting results were evaluated by root-mean-square-error (RMSE) which is a statistical measure of residuals between the data and estimated values.

$$C(R,t) = \frac{1}{2}\left\{erfc\left(\frac{R - v^s t}{2\sqrt{D_x^s t}}\right) + \exp\left(\frac{R v^s}{2\sqrt{D_x^s t}}\right) erfc\left(\frac{R + v^s t}{2\sqrt{D_x^s t}}\right)\right\} \tag{10}$$

3. RESULTS AND DISCUSSIONS

Firstly, the analyses for the transport in flow direction were carried out to evaluate transport parameters. In case of solute tracer tests, BTCs observed from the three EC sensors except the source point were analyzed for 18 tests. And four temperature BTCs obtained by four RTD sensors were analyzed for 34 tests. Applying Eqs. 9 and 10 to the BTCs was performed by minimizing the sum of squares of deviations in previous stage. In the results, the minimum RMSE values were 0.010 and 0.020 for the solute and tracer tests and this means that the fitted data matched well with the monitored data. The best fit results are shown in Fig. 3.

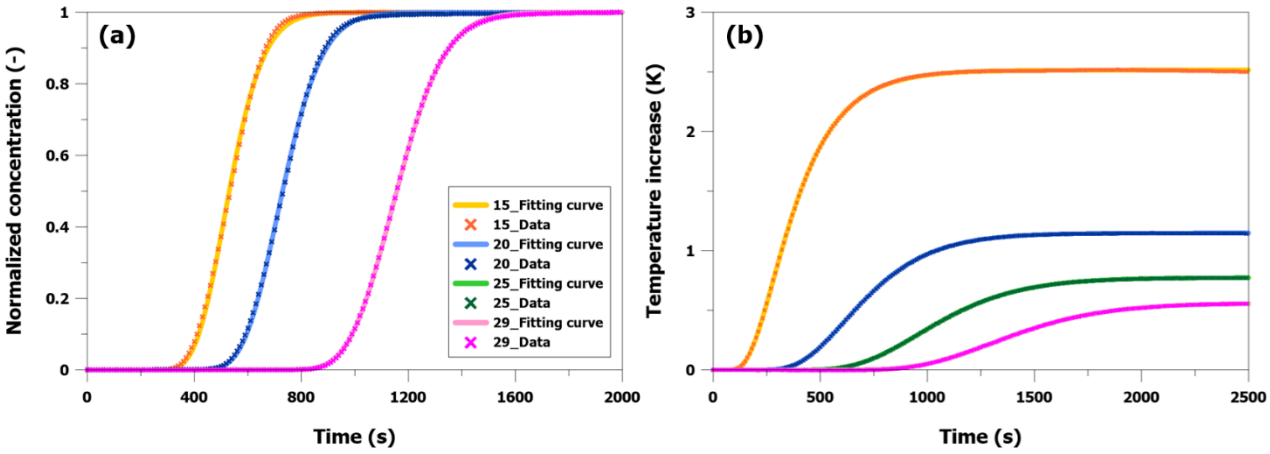

Figure 3: The best fit results of forward models. The solid lines represent fitted curve by forward model and the marks represent observed data at each monitoring point. (a) Solute forward model. and (b) Heat forward model.

Front velocities estimated by SFM is much larger than those estimated by HFM despite identical background flow velocities. One of the reasons why the two velocities are different is that solute tracer can flow into the pore space only unlike heat tracer. Solute front velocities estimated by SFM were overall underestimated than velocities calculated by Eq. 1. Thermal front velocities evaluated by HFM were also underestimated and the difference between the velocities are much larger than the results of SFM. The maximum difference at the sensor 29 which is closest from the outlet tank, is up to 10% for the solute front velocities and 30% for the thermal front velocities (Figs. 4 and 5)

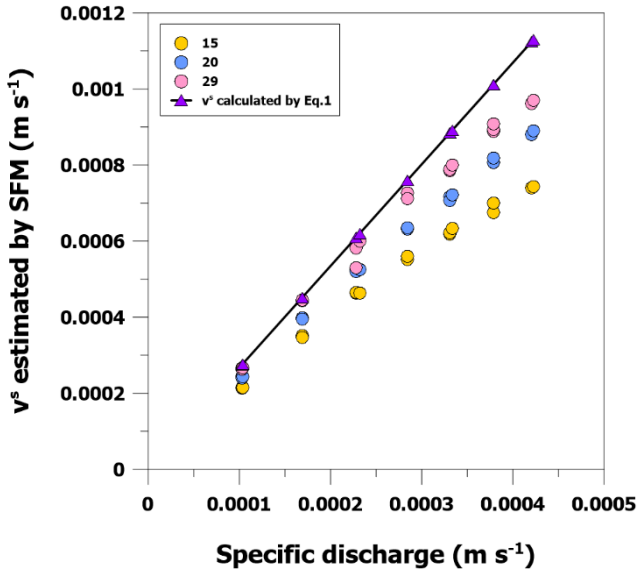

Figure 4: Specific discharge measured from the outlet tank during each experiment versus solute front velocities estimated by SFM for 18 tests.

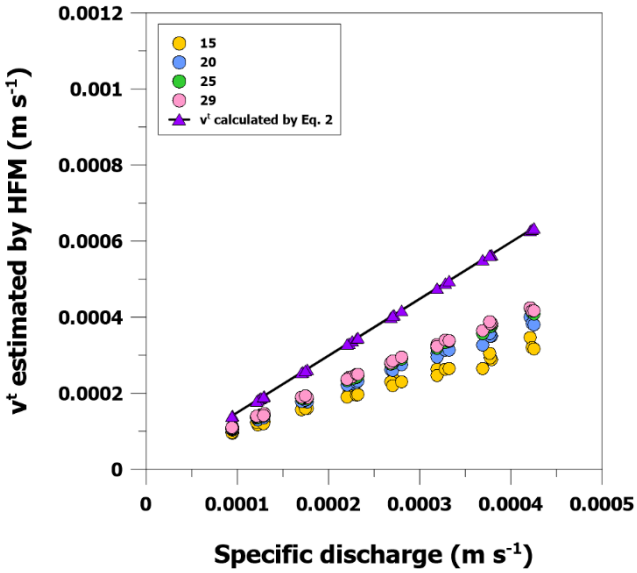

Figure 5: Specific discharge measured from the outlet tank during each experiment versus thermal front velocities estimated by HFM for 34 tests.

While tracer front velocities showed the similar trend each other, the relationship between front velocities and dispersion coefficients are different in solute and heat. The range of dispersion coefficient is a little larger in solute than heat, and the different range along the location is also appeared in both tracers as shown in Figs. 6 and 7. Solute front velocities and dispersion coefficients show a clear linear trend, but the relationship between thermal front velocities and dispersion coefficients can be explained by a power law which has higher R-squared value than those of a linear relationship or a square law. These different types of curves can be explained by different transport regimes. In this study, solute Peclet number ($Pe^s < 141.33$) is much larger than thermal Peclet number ($Pe^t < 0.71$) even under the same background flow conditions.

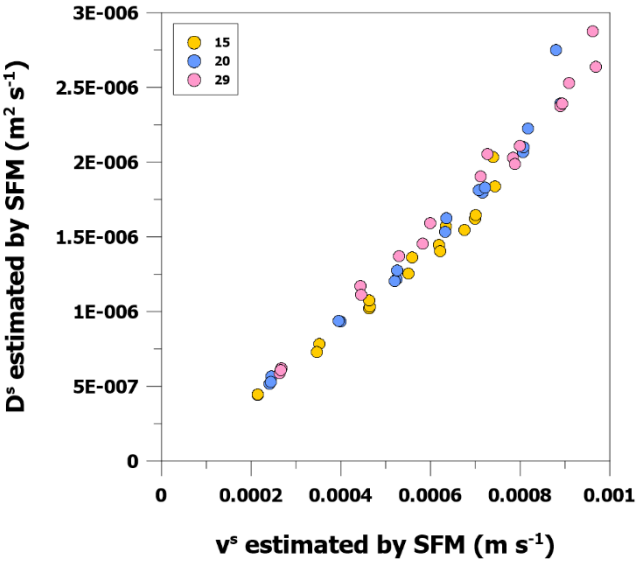

Figure 6: The velocity dependency of longitudinal solute dispersion coefficients.

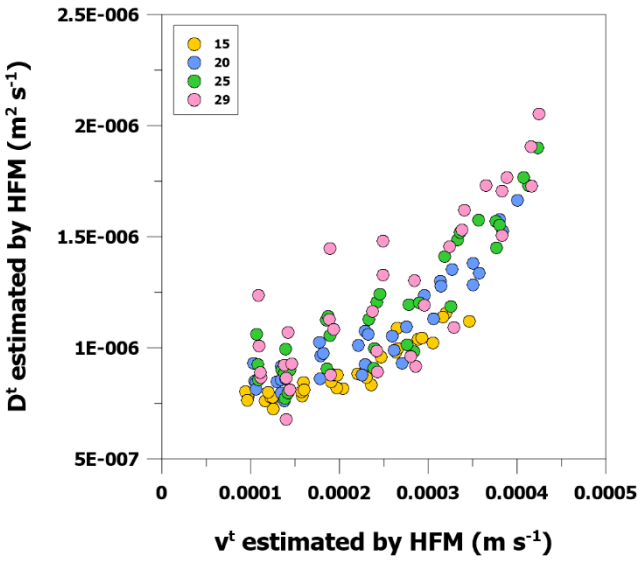

Figure 7: The velocity dependency of longitudinal thermal dispersion coefficients.

4. CONCLUSION

In this study, heat and solute tracer tests were conducted with the laboratory experimental device under various flow fields. The solute and thermal behaviors in the porous medium were interpreted by mathematical models. The fittings between analytical solutions and BTCs were carried out by nonlinear least square method and the results were evaluated by RMSE. Theoretical behaviors from SFM and HFM were matched well with time series data measured. Solute and thermal front velocities are in different transport regimes under the same background flow velocities due to their physical differences, and both velocities estimated by forward models were underestimated than those derived from Eqs. 1 and 2. Dispersion coefficients showed different dependencies for respective front velocities, but their magnitudes were in a similar range. Through the comparisons, the differences between transport parameters caused by their physical differences were identified.

5. ACKNOWLEDGMENTS

This work was supported by the National Research Foundation of Korea (NRF) grant funded by the Ministry of Science and ICT (MSIT) of South Korean government (No. 2017R1A2B3002119). This subject was also supported by National Research Foundation of Korea (NRF) grant funded by the Korea government (MIST) (0409-20190119).

6. NOMENCLATURE

d_{50}	mean grain size [m]
C_u	coefficient of uniformity [-]
n_e	effective porosity [-]
ρ	density [kg m^3]
K	hydraulic conductivity [m s^{-1}]
q	specific discharge [m s^{-1}]
μ	dynamic viscosity [kg m^{-1} s^{-1}]
λ	thermal conductivity [W m^{-1} K^{-1}]
ρc	heat capacity [J m^3 K^{-1}]
Re	Reynolds number [-]
Pe	Peclet number [-]
C	concentration [kg m^{-3}]
T	temperature [℃]
D	dispersion coefficient of tracer [m^2 s^{-1}]
v	front velocity of tracer [m s^{-1}]
M	source of mass flow [g s^{-1}]

Q source of heat flow [W]

t time [s]

R $\sqrt{\mathrm{x}^2 + \frac{D_x^{s,t}}{D_y^{s,t}}(y^2 + z^2)}$ [m]

Supscripts

t thermal

s solute

Subscripts

x x direction of Cartesian coordinate

y y direction of Cartesian coordinate

z z direction of Cartesian coordinate

s properties of sand

w properties of water

b properties of bulk porous medium

REFERENCES

Bandai, T., Hamamoto, S., Rau, G. C., Komatsu, T. and Nishimura, T.: The effect of particle size on thermal and solute dispersion in saturated porous media. International Journal of Thermal Sciences, 122, (2017), 74-84.

de Marsily, G.: Quantitative hydrogeology, Academic, San Diago, (1986), pp.440.

Hunt, B.: Dispersive sources in uniform ground-water flow, Journal of the Hydraulics Division, 104(1), (1978), 78-85.

Ma, R., Zheng, C., Zachara, J. M. and Tonkin, M.: Utility of bromide and heat tracers for aquifer characterization affected by highly transient flow conditions. Water Resources Research, 48(8), (2012), W08523.

Park, B. H., Bae, G. O. and Lee, K. K.: Importance of thermal dispersivity in designing groundwater heat pump (GWHP) system: Field and numerical study, Renewable energy, 83, (2015), 270-279.

Park, B. H., Lee, B. H. and Lee, K. K.: Experimental investigation of the thermal dispersion coefficient under forced groundwater flow for designing an optimal groundwater heat pump (GWHP) system, Journal of hydrology, 562, (2018), 385-396.

Piga, B., Casasso, A., Pace, F., Godio, A. and Sethi, R.: Thermal impact assessment of groundwater heat pumps (GWHPs): Rigorous vs. simplified models, Energies, 10(9), (2017), 1385.

Rau, G. C., Andersen, M. S. and Acworth, R. I.: Experimental investigation of the thermal dispersivity term and its significance in the heat transport equation for flow in sediments, Water Resources Research, 48(3), (2012), W03511.

Sarris, T. S., Close, M., and Abraham, P: Using solute and heat tracers for aquifer characterization in a strongly heterogeneous alluvial aquifer, Journal of hydrology, 558, (2018), 55-71.

Schincariol, R. A. and Schwartz, F. W.: An experimental investigation of variable density flow and mixing in homogeneous and heterogeneous media, Water Resources Research, 26(10), (1990), 2317-2329.

Vandenbohede, A., Louwyck, A. and Lebbe, L.: Conservative solute versus heat transport in porous media during push-pull tests. Transport in Porous Media, 76(2), (2009), 265-287.